Journal of the Nigerian Association of Mathematical Physics
***Volume* 16 (May, 2010), pp 57 - 68**

Surface energy calculation of fcc metals using the new analytical algorithm for equivalent crystal theory

S Yusuf [1] E Aghemenloh [2,]*, J O A Idiodi[3]
[1] Department of Science Laboratory, Kogi State Polytechnic, Lokoja, Kogi State, Nigeria.
[2] Department of Physics, University of Benin, Benin City, P.M.B. 1154, Edo State, Nigeria.
[3]Corresponding author: email jidiodi@hotmail.com Tel. +2348037994106

Abstract

The surface energies of 3 surfaces of 13 fcc metals have been calculated using the new analytical algorithm for equivalent crystal theory (ECT). This is an extension of the work of Zypman and Ferrante which reported surface energy results for only the (100) surface of seven fcc metals. Our results show that, for all the fcc metals, the surface energies of (110) are higher than that of the (100) and the (111) surfaces. The present surface energy results compares well with the available energy results of Zypman and Ferrante. And also, in good agreement with an earlier surface energy results of Aghemenloh and Idiodi using the old ECT. The ordering of the three low-index surface energies is $\sigma_{111} < \sigma_{100} < \sigma_{110}$, ***in agreement with other theoretical results. Thus, the (111) plane has the lowest energy. Generally, our computed results are in good agreement with the results of both experiment and first principles calculations.***

1.0 Introduction

Surface energy is an important physical quantity. Many surface phenomena such as reconstruction, adsorption, shape transition in nanoscale particles, alloying, epitomical growth, oxidation, corrosion, catalysis, crystal growth [1-5], etc are directly related to the structure and energy of surfaces [6,7]. So it is necessary to know the surface energies for various surfaces. However, determination of surface energy is fraught with problems. The first is that experimental measurements are more commonly found for polycrystalline materials which are subject to errors due to surface-active contaminants. Secondly, experimental values are not generally available, and in those cases where they are, the experimental predictions vary widely. Thirdly, in the last few years, in spite of increasing effort on first principle calculations, first principle results are plagued with instabilities and lack of convergence. To avoid these problems and especially the heavy computation involved in ab initio methods, Semi-empirical methods [8-11] were developed.

A semi-empirical approach to the many-body problem consists in determining a functional form for the cohesive energy based on a physical model. This function is fitted to experimental results to estimate the parameters required for complete description. This explicit function is in turn used to calculate some other material properties like defect energies etc. Various semi-empirical models derived in this manner have been successful in describing a wide range of material properties [8-11]. However, surface energies predicted by some of these models are significantly lower than reported experimental values or results from ab initio calculations. A major drawback in some of these semi-empirical methods is the lack of experimental values for the basic inputs like the vacancy formation energies and the associated uncertainties in the cases where they are available.

The equivalent crystal theory method (ECT) since its introduction have been extensively used to describe the energetic of defects in metals [12, 13] and alloys [14, 15], and also in the study of charge transfer in metal nano-clusters [16]. More recently the ECT was extended to hcp metals to calculate surface energies [17]. However, the major constraint in the implementation of the ECT method at present is the time limiting step involved in finding the root of the equations

which might be important for complex defects and large systems.
To overcome this constraint, recently Zypman and Ferrante [18] introduced an analytical algorithm to invert the ECT equations that reduces the computational speed by employing the Lambert function. This new algorithm of the ECT has successfully been applied to calculate the (100) surface energy of seven fcc metals. The aim of this study therefore, is to extend the surface energy results of Zypman and Ferrante [18] from the seven fcc metals to other important fcc metals in the literature, and also to include the two other low-index crystal faces, the (110) and (111) faces.
The remainder of this paper is organized as follows. In section 2, we give a brief discussion of the new analytical ECT method. In section 3, we discuss the analytical ECT method of calculating the surface energies of fcc metals. The results of surface energies for 13 fcc metals are reported in section 4, along with the results obtained by other workers. Concluding remarks are giving in section 5.

2. The New Analytical ECT Method

In ECT the total energy of a collection of atoms in a defect is the sum of individual energy contributions $U(a_{eq})$, where a_{eq} is called equivalent lattice parameter and $U(a_{eq})$, is explicitly given by the Universal binding energy relation (UBER) [19] which is simply parameterized in terms of physically known constants in the Rydberg function. In ECT an atom near a defect is viewed as sensing a reduced or increased electron density. This condition is then interpreted as a point on the UBER in terms of an expanded or contracted perfect crystal. Perturbation theory is used to obtain the equivalent lattice parameter of the expanded or contracted crystal, a_{eq} in terms of a_0 the lattice parameter corresponding to the perfect crystal. Once a_{eq} is known, the energy of the atom near the defect is obtained from that point on the UBER. The value of a_{eq} is obtained in terms of a_0 from the inversion of the basic ECT transcendental equation. Although conceptually simple, the inversion process represents the computational time limiting step in the implementation of the algorithm.

The implementation of ECT involves a perturbation equation that determines the energy of a solid with a defect in terms of a perfect crystal of the same substance expanded or contracted from the equilibrium lattice parameter to a new "equivalent" lattice parameter. This procedure is equivalent to finding an embedding electron density ρ. A typical atom at a given location is embedded in a density ρ produced by the electronic charge density of the remainder atoms in the system. The yet unknown, equivalent nearest-neighbour distance, R_{eq} satisfies

$$N_1 R_{eq}^p e^{-\alpha R_{eq}} + N_2 \left(C_2 R_{eq}\right)^p e^{-\left(\alpha+\frac{1}{\lambda}\right)C_2 R_{eq}} = \rho \qquad (1.0)$$

where N_1 is the number of nearest – neighbours in the minimum energy crystal structure corresponding to that atom, N_2 is the number of next-nearest neighbours, C_2 is the ratio of the next-nearest-neighbour distance to the nearest-neighbour distance, and α and λ are known material-dependent constants. In many applications of ECT to evaluate defect formation energies, ρ, on the right-hand side of Eq. (1.0), is written in a form similar to the left-hand side. For example, the density produced by neighbours on an atom next to a vacancy is

$$\rho = N_1^1 R_0^p e^{-\alpha R_0} + N_2^1 \left(C_2 R_{eq}\right)^p e^{-\left(\alpha+1/\lambda\right)C_2 R_0},$$

where $N_1^1 = N_1 - 1$ and $N_2^1 = N_2$ because the atom in question loses one nearest-neighbour (where the vacancy is located) and no second near neighbour. In this example, the lattice is unrelaxed and consequently R_0 represents the nearest neighbour distance of the perfect crystal. This shows explicitly that R_{eq} is the unknown in Eq. (1.0). Once R_{eq} is obtained, ECT used this value in the UBER function, $U(a_{eq})$. The corresponding energy cost is then $U(a_{eq}) - U(a_o)$. In what follows, we adopt the method of Zypman and Ferrante [18].

The general problem is therefore to find the function

$$R_{eq} = G(\rho) \qquad (2.0)$$

Equation (1.0) can be cast in dimensionless form by defining

$$y \equiv \alpha R_{eq}$$

$$y^p e^{-y} + \frac{N_2}{N_1} C_2^p y^p e^{-\left(1+1/\alpha\lambda\right)C_2 y} = \frac{\rho\alpha^p}{N_1} \tag{3.0}$$

By introducing $\left(1+\frac{1}{\alpha\lambda}\right)C_2 - 1 \equiv \gamma$, $\frac{N_2}{N_1} \equiv n_{21}$, $\frac{\rho\alpha^p}{N_1} \equiv x$, Eq. (3.0) becomes

$$y^p e^{-y}\left(1 + n_{21} c_2^p y^p e^{-\gamma y}\right) = x \tag{4.0}$$

The constant $\alpha\lambda$ is about unity or larger and $C_2 > 1$, thus $\gamma > 0$, which is a conservative lower bound for γ. By using appropriate values from Table 1, one finds that $n_{21} c_2^p y^p e^{-\gamma y} < 0.04$ as earlier reported [18]. Thus, in Eq. (4.0), the second term inside the parenthesis is much smaller than unity, and therefore it is dropped in many real applications. Thus, the problem reduces to finding the roots of

$$y^p e^{-y} = x \tag{5.0}$$

A sketch of Eq. (5.0) is shown in Fig.1. In Fig.1, the root y_1 corresponds to the smaller lattice parameter while the root y_2 corresponds to the larger lattice parameter. Creating a vacancy effectively lowers the atom density thereby increasing y [8]. Thus the physically accepted root is y_2.

Equation (5.0) can now be recast in the Lambert form:

$$\left(\frac{-y}{p}\right) e^{\left(\frac{-y}{p}\right)} = \frac{-x^{1/p}}{p} \tag{6.0}$$

with the solution

$$y = -pW_{-1}\left(\frac{-x^{1/p}}{p}\right) \tag{7.0}$$

where W_{-1} is the Lambert function [20, 21]. The sub index "-1" labels the branches. The Lambert function has an infinite number of complex branches with only two purely real, the branches known as "0" and "-1".

Define (y_m, x_m) as the point corresponding to the maximum attainable density. y_M may be found by taking the maxima of Eq. (4.0) as

$$P - y_M + n_{21} c_2^p e^{-\gamma y_M}\left[P - (1+\gamma) y_M\right] = 0 \tag{8.0}$$

Eq. (8.0) can be solved for γ as

$$\gamma \equiv \Omega^{-1}(y_M) = \frac{1}{y_M}\left[p - y_M - w_0\left(\frac{-(p - y_M)e^{p - y_M}}{n_{21} c_2^p}\right)\right] \tag{9.0}$$

Again, taking the inverse of the maxima of Eq. (9.0) to obtain y_M , we have

$$(p - y_{Mm})y_{Mm}^2\left[1 + W_0\left(\frac{(y_{Mm} - P)e^{P - y_{Mm}}}{n_{21}c_2^p}\right)\right] = 0 \tag{10.0}$$

The only non-trivial solution to Eq. (10.0) is for the argument of the Zero branch to be -1/e. For a complete discussion of the above equations and the conditions that lead to its derivations, the interested reader is referred to the work of Zypman and Ferrante [18], where the details can be found. According to Zypman and Ferrante, the smallest possible value of *y (*y_{min}*)* is given as

$$y_{\min} = P - W_0(n_{21}\frac{c_2^p}{e}) \tag{11.0}$$

Eq.(11.0) was used to evaluate the y_{min} in Table 2.

3.0 Calculation of Surface Energy

Here, we implement the analytical algorithm of the ECT by Zypman and Ferrante. The surface energies of the three low-index planes of thirteen fcc metals is obtained by this algorithm. However, it is emphasize that only the volume term of the ECT is retained, while neglecting the other terms. The neglect of the higher order terms of the ECT has been justified from previous studies [17, 22, 23]. In what follows we first solve Eq.(4.0) numerically, and then by the Lambert function as given by [18].

For the real density of the (111) plane, we notice that a typical surface atom losses 3 nearest-neighbours (out of 12 in bulk) and 3 next nearest-neighbours (out of 6 in the bulk). Then

$$\rho = 9R_0^p\exp(-\alpha R_0) + 3(C_2R_0)^p\exp\left[-\left(\alpha + \frac{1}{\lambda}\right)C_2R_0\right] \tag{12.0}$$

where α, ρ and λ are material constants whose values depends on each metal. And C_2 and R_0 are given as $R_0 = \frac{a}{\sqrt{2}}$, $c_2 = \sqrt{2}$. Solving eq. (12), we obtain the value of electron density ρ

Next, we solve

$$x = \frac{\rho\alpha^p}{12} \tag{13.0}$$

and then

$$y = -p\,\mathrm{Pr}oduct\,Log\left[-1, \frac{-x^{1/p}}{p}\right] \tag{14.0}$$

Now, after obtaining the value of x from Eq. (13.0), we then compute the nearest neighbour distance R_{eq} from the relation

$$R_{eq} = \frac{y}{\alpha} \tag{15.0}$$

Once the value of y has been obtained from Eq.(14.0) and knowing the value of the material constant α, we can then calculate the value of R_{eq} from Eq. (15.0). Next, we compute the lattice parameter a_{eq} from

$$a_{eq} = C_2R_{eq} \tag{16.0}$$

For the real density of the (110) plane, two surfaces are involved, the surface plane (j = 1) and the first surface below the surface plane (j=2). The equations for ρ to be solved are:

$$\rho = 7R_0^p\exp(-\alpha R_0) + 4(C_2R_0)^p\exp\left[-\left(\alpha + \frac{1}{\lambda}\right)C_2R_0\right] \tag{17.0a}$$

and

$$\rho = 11R_0^p\exp(-\alpha R_0) + 4(C_2R_0)^p\exp\left[-\left(\alpha + \frac{1}{\lambda}\right)C_2R_0\right] \tag{17.0b}$$

The real density of the (100) plane also involves two surfaces like in the case of the (110) plane. The surface atom losses 4 nearest – neighbours and 1 next nearest-neighbour atom for the surface plane (j=1),

while the second plane (j=2) losses only 1 next nearest – neighbour atom. Therefore, the equations to be solved are:

$$\rho = 8R_0^p \exp(-\alpha R_0) + 5(C_2 R_0)^p \exp\left[-\left(\alpha + \frac{1}{\lambda}\right) C_2 R_0\right] \tag{18.0a}$$

and

$$\rho = 12R_0^p \exp(-\alpha R_0) + 5(C_2 R_0)^p \exp\left[-\left(\alpha + \frac{1}{\lambda}\right) C_2 R_0\right] \tag{18.0b}$$

Eqs(17.0) and (18.0) are then solved for ρ and Eqs.(13.0) and (14.0) for x and y. Thereafter, Eqs.(15.0) and (16.0) are solved for R_{eq} and a_{eq} for each fcc metals.

Once the values of R_{eq} are known from Eq. (15.0), then the values of a^* and F^* can be calculated directly [8]. The surface energy for each of the three low-index faces is then calculated from the formulas

$$\sigma_{111} = \frac{4}{a^2\sqrt{3}} \Delta E \sum_j F^*[a^*, (j)] \tag{19.0}$$

$$\sigma_{110} = \frac{\sqrt{2}}{a^2} \Delta E \sum_j F^*[a^*, (j)] \tag{20.0}$$

$$\sigma_{100} = \frac{2}{a^2} \Delta E \sum_j F^*[a^*, (j)] \tag{21.0}$$

The sum over j includes only one atom per atomic layer, and usually only a few layer need be included for metal low index planes.

4. Results and Discussion

The equivalent crystal nearest neighbour distance R_{eq} is a very vital parameter in the ECT method, since it is the parameter needed in the calculation of surface energy. R_{eq} values are also needed in the computation of a_{eq}, the equivalent lattice parameters. These are shown in Table 3 and have been employed to calculate the values of surface energies exhibited in Table 4. Table 3 also displays the relative difference between the Lambert evaluation method (AECT) and the numerical evaluation (Newton –Raphson method) of the ECT. Table 3 provides a comparison of this present work using Lambert evaluation with a previous work by Zypman and Ferrante [18] and other previous studies [24,25] which used the original ECT. It can be seen from the table that there is a good agreement between the two ECT methods. Like in Table 3, the present AECT results of surface energies in Table 4 compares well with the results of Zypman and Ferrante where results are available. The results are also in good agreement with the earlier work of Aghemenloh and Idiodi [24].

The summary of our surface energies obtained for the three low – index faces of the thirteen fcc metals using the New ECT method are presented in Table 5. These results are then compared with the results from first principles calculations [26-28] the tight – binding (TB) method [29] , the embedded atom method (EAM) [30,31], the modified embedded atom method (MEAM)[32],the modified analytical embedded atom method (MAEAM) [33], and experiment [34]. For all the theoretical models whose results are presented in table 5, the closed – packed (111) face has the lowest energy. It is important to note that while the AECT, TB, EAM, MAEAM and the first principles results consistently support the trend $\sigma_{111} < \sigma_{100} < \sigma_{110}$, the results of the MEAM in Table 5 do not always support this trend. In a few cases the low density (110) surface energy is higher than the (100) surface energy. The AECT surface energies are uniformly larger and closer to experiment than those obtained by the EAM, which is known to under estimate surface energies in fcc metals [8, 29, 22]. The surface energies from this study are generally closer to experiment than those obtained by the MEAM [32], MAEAM [33] and TB [29] and in good agreement with first principles calculations [26-28].

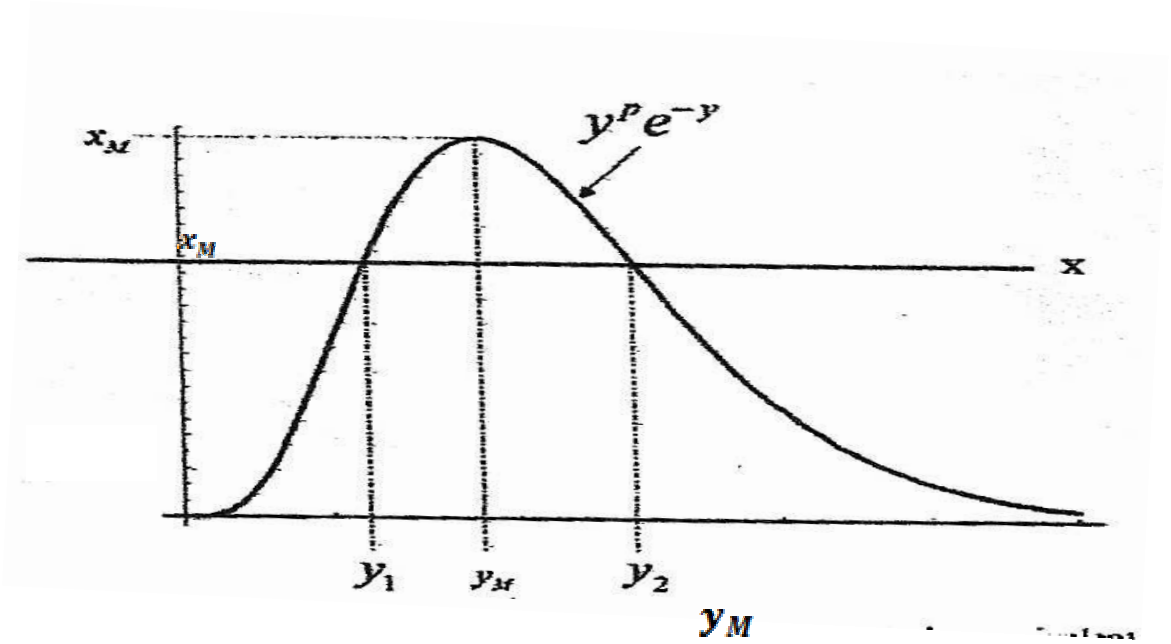

Fig. 1. shows Eq. (5) graphically illustrating the appearance of two roots: The root y_1 is to the left of the maximum that correspond to a lattice parameter smaller than a_0,while the root y_2 to the right corresponds to the lattice parameter larger than a_0.

Table 1. Pure metal properties and the calculated ECT constants for fcc metals. All input parameters were taken from the work of Aghemenloh and Idiodi [24].

Element	Cohesive energy ΔE(eV)	Lattice constant a(Å)	E^f_{1v} (eV)	Bulk Modulus($10^{11}Jm^{-3}$)	p	l(Å)	λ(Å)	α($Å^{-1}$)	$r_{WSE(Å)}$
Ni	4.44	3.51	1.60	1.876	6	0.271	0.761	3.013	1.372
Pd	3.94	3.89	1.40	1.955	8	0.237	0.667	3.611	1.520
Pt	5.85	3.92	1.30	2.884	10	0.237	0.667	4.534	1.532
Cu	3.50	3.61	1.30	1.420	6	0.272	0.766	2.934	1.411
Ag	2.96	4.08	1.19	1.087	8	0.269	0.757	3.334	1.594
Au	3.78	4.07	0.96	1.803	10	0.237	0.665	4.336	1.590
Al	3.34	4.04	0.66	0.794	4	0.336	0.946	2.104	1.579
Pb	2.04	4.95	0.	0.488	10	0.303	0.852	3.539	1.937
Rh	5.75	3.80	1.71	2.704	8	0.247	0.693	3.726	1.485
Ca	1.84	5.58	0.6	0.152	6	0.486	1.365	1.864	2.181
Sr	1.72	6.08	0.6	0.116	8	0.515	1.447	2.160	2.376
Ir	6.94	3.84	2.35	3.704	10	0.2530	0.647	4.417	1.501
Th	6.20	5.08	2.0	0.543	12	0.494	1.389	3.617	1.985

Table 2. Smallest value of Y $(= y_{min})$ and corresponding γ values for thirteen fcc metals.

Element	Y_{min}	$\gamma = \left(1 + \frac{1}{\alpha\lambda}\right) C_2 - 1$	$Z \equiv n_{21} c^p e^{-\gamma y}$
Ni	5.282	1.032	0.017
Pd	6.960	1.002	0.007
Pt	8.579	0.882	0.008
Cu	5.282	1.044	0.016
Ag	6.960	0.975	0.009
Au	8.579	0.906	0.007
Al	3.537	1.126	0.037
Pb	8.579	0.883	0.008
Rh	6.960	0.962	0.010
Ca	5.282	0.970	0.024
Sr	6.960	0.867	0.019
Ir	8.579	0.909	0.066
Th	10.150	0.696	0.027

Table 3. ECT equivalent lattice parameters, and the relative difference between Lambert evaluation (AECT) and numerical evaluation (ECT).

Element	Crystal face (hkl)	a_{eq} (Å) (Present)	a_{eq} (Å)[a]	a_{eq} (Å)[b]	Δa_{eq} (Å)

	Ni	(100)	4. 213	4.21	4.214		0.001	
		(110)	4.394		4.395		0.001	
		(111)	4.041		4.042		0.001	
	Pd	(100)	4.516	4.52	4.517		0.001	
		(110)	4.680		4.681		0.001	
		(111)	4.359		4.360		0.001	
	Pt	(100)	4.422	4.42	4.422		0	
		(110)	4.549		4.559		0.01	
		(111)	4.293		4.294		0.001	
	Cu	(100)	4.331	4.33	4.332		0.001	
Ni		(100)	(110)	3.125	4.517	1.203	4.517	1.22[a]	3.123[b]	0[b]	1.202[b]
		(110)	(111)	3.231	4.154	1.759	4.155		3.234[b]	0.001[b]	1.761[b]
	Ag	(111)	(100)	2.396	4.808	0.799	4.811		2.398[b]	0.003[b]	0.799[b]
Pd		(100)	(110)	2.303	4.992	1.089	4.995	1.10[a]	2.302[b]	0.003[b]	1.089[b]
		(110)	(111)	2.381	4.632	1.592	4.634		2.381[b]	0.002[b]	1.592[b]
	Au	(111)	(100)	1.752	4.604	0.717	4.605		1.752[b]	0.001[b]	0.717[b]
Pt		(100)	(110)	2.458	4.747	1.180	4.749	1.31[a]	2.457[b]	0.002[b]	1.1798[b]
		(110)	(111)	2.607	4.467	1.771	4.469		2.608[b]	0.002[b]	1.771[b]
	Al	(111)	(100)	1.790	4.740	0.744	4.742		1.791[b]	0.002[b]	0.7448[b]
Cu		(100)	(110)	2.395	4.942	0.971	4.944	0.98[a]	2.395[b]	0.002[b]	0.971[b]
		(110)	(111)	2.463	4.554	1.418	4.557		2.465[b]	0.003[b]	1.4197[b]
	Pb	(111)	(100)	1.833	5.617	0.646	5.617		1.835[b]	0[b]	0.647[b]
Ag		(100)	(110)	1.638	5.795	0.847	5.795	0.84[a]	1.632[b]	0[b]	0.849[b]
		(110)	(111)	1.673	5.448	1.231	5.448		1.678[b]	0[b]	1.234[b]
	Rh	(111)	(100)	1.262	4.396	0.568	4.397		1.266[b]	0.001[b]	0.570[b]
Au		(100)	(110)	1.620	4.554	0.838	4.554	0.89[a]	1.620[b]	0[b]	0.838[b]
		(110)	(111)	1.706	4.246	1.249	4.247		1.706[b]	0.001[b]	1.249[b]
	Ca	(100)		6.754			6.756		0.002		
		(110)		7.052			7.053		0.001		
		(111)		6.471			6.474		0.003		
	Sr	(100)		7.304			7.306		0.002		
		(110)		7.599			7.600		0.001		
		(111)		7.021			7.023		0.002		
	Ir	(100)		4.420			4.421		0.001		
		(110)		4.569			4.569		0		
		(111)		4.278			4.278		0		
	Th	(100)		6.079			6.080		0.001		
		(110)		6.296			6.296		0		
		(111)		5.868			5.870		0.002		

[a] New ECT method, using analytical Lambert evaluation .[18]
[b] Old ECT method, using numerical evaluation .[24, 25]

$$\Delta a_{eq}(\text{Å}) = (a^{b}_{eq_{Numerical}} - a^{a}_{eq_{Lambert}})/a^{b}_{eq_{Numerical}}$$

Table 4. Rigid surface energies for low-index fcc metals

	(111)	1.193	0.535		1.193 [b]	0.535 [b]
Al	(100)	1.286	0.656	0.73 [a]	1.289 [b]	0.657 [b]
	(110)	1.384	0.998		1.387 [b]	1.000 [b]
	(111)	0.918	0.406		0.922 [b]	0.407 [b]
Pb	(100)	0.568	0.435		0.568 [b]	0.435 [b]
	(110)	0.599	0.649		0.599 [b]	0.649 [b]
	(111)	0.419	0.278		0.419 [b]	0.278 [b]
Rh	(100)	3.105	1.401		3.112 [b]	1.404 [b]
	(110)	3.243	2.070		3.251 [b]	2.075 [b]
	(111)	2.325	0.909		2.333 [b]	0.912 [b]
Ca	(100)	0.461	0.448		0.462 [b]	0.449 [b]
	(110)	0.480	0.660		0.483 [b]	0.665 [b]
	(111)	0.353	0.298		0.356 [b]	0.300 [b]
Sr	(100)	0.355	0.410		0.355 [b]	0.410 [b]
	(110)	0.368	0.601		0.369 [b]	0.603 [b]
	(111)	0.277	0.277		0.277 [b]	0.277 [b]
Ir	(100)	3.907	1.801		3.898 [b]	1.796 [b]
	(110)	4.046	2.637		4.040 [b]	2.633 [b]
	(111)	2.978	1.188		2.971 [b]	1.186 [b]
Th	(100)	1.445	1.166		1.443 [b]	1.164 [b]
	(110)	1.507	1.718		1.510 [b]	1.722 [b]
	(111)	1.154	0.806		1.155 [b]	0.807 [b]

Element	Crystal face (hkl)	AECT (Jm^{-2}) (Present)	AECT (eV/atom) (Present)	AECT (eV/atom)	ECT (Jm^{-2})	ECT (eV/atom)

[a] New ECT method, using analytical Lambert evaluation .[18]
[b] Old ECT method, using numerical evaluation .[24, 25]

Table 5. Experimental and theoretical surface energies (in Jm^{-2}) for FCC Metals

Element	Crystal face (hkl)	AECT (Present)	First Principles Calculations	TB[d]	MEAM[e]	EAM	MAEAM[h]	Expt[i]
Ni	(100)	3.125	2.426[C]		2.435	1.580[f], 1.654[g]	1.304	
	(110)	3.231	2.368[C]		2.384	1.730[f], 1.786[g]	1.417	
	(111)	2.396	2.630[a] 2.011[C]		2.036	1.450[f], 1.540[g]	1.170	2.450
Pd	(100)	2.303	1.900[a], 1.860[b], 2.326[C]	1.750	1.659	1.370[f], 1.157[g]	1.018	
	(110)	2.381	1.970[b], 2.225[C]	1.860	1.470	1.490[f], 1.240[g]	1.119	
	(111)	1.752	1.880[a], 1.640[b], 1.920[C]	1.570	1.381	1.220[f], 1.074[g]	0.926	2.050
Pt	(100)	2.458	2.480[a], 2.734[C]	2.830	2.167	1.650[f], 1.228[g]	1.079	
	(110)	2.607	2.819[C]	2.970	2.131	1.750[f], 1.309[g]	1.188	
	(111)	1.790	2.350[a], 2.299[C]	2.510	1.656	1.440[f], 1.120[g]	0.902	2.480
Cu	(100)	2.385	2.090[a], 2.166[C]	1.930	1.651	1.280[f], 1.260[g]	1.006	
	(110)	2.463	2.310[a], 2.237[C]	2.040	1.642	1.400[f], 1.361[g]	1.106	
	(111)	1.833	1.960[a], 1.952[C]	1.730	1.409	1.170[f], 1.180[g]	0.939	1.830
Ag	(100)	1.628	1.200[a], 1.210[b], 1.200[C]	1.290	1.271	0.705[f], 1.821[g]	0.752	
	(110)	1.673	1.290[a], 1.266[b], 1.238[C]	1.420	1.222	0.770[f], 1.883[g]	0.833	
	(111)	1.262	1.120[a], 1.210[b], 1.172[C]	1.140	1.089	0.625[f], 0.765[g]	0.713	1.250
Au	(100)	1.620	1.710[a], 1.627[c]	1.690	1.084	0.918[f], 0.683[g]	0.713	
	(110)	1.706	1.790[a], 1.700[c]	1.850	1.115	0.980[f], 0.728[g]	0.794	
	(111)	1.193	1.610[a], 1.283[C]	1.480	0.886	0.790[f], 0.618[g]	0.640	1.500
Al	(100)	1.286	1.347[C]		0.877	0.579[g]	0.476	
	(110)	1.384	1.271[C]		0.969	0.627[g]	0.515	
	(111)	0.918	1.270[a], 1.199[C]		0.618	0.524[g]	0.396	1.160
Pb	(100)	0.568	0.377[C]		0.424			
	(110)	0.599	0.445[C]		0.431			

	(111)	**0.419**	**0.321[C]**		**0.366**		**0.600**
Rh	**(100)**	**3.105**	**2.900[a], 2.810[b], 2.799[C]**	**2.570**	**2.902**	**2.137**	
	(110)	**3.243**	**2.880[b], 2.899[C]**	**2.710**	**2.921**	**2.272**	
	(111)	**2.325**	**2.780[a], 2.530[b], 2.472[C]**	**2.460**	**2.598**	**1.834**	**2.700**
Ca	**(100)**	**0.461**	**0.542[C]**				
	(110)	**0.480**	**0.582[C]**				
	(111)	**0.353**	**0.352[a], 0.567[C]**				**0.490**
Sr	**(100)**	**0.355**	**0.408[C]**				
	(110)	**0.368**	**0.432[C]**				
	(111)	**0.277**	**0.287[a], 0.428[C]**				**0.410**
Ir	**(100)**	**3.907**	**3.722[C]**	**2.950**	**2.907**	**2.569**	
	(110)	**4.046**	**3.606[C]**	**3.190**	**3.058**	**2.664**	
	(111)	**2.978**	**2.971[C]**	**2.590**	**2.835**	**2.038**	**3.000**
Th	**(100)**	**1.445**	**1.468[C]**				
	(110)	**1.507**	**1.450[C]**				
	(111)	**1.154**	**1.476[C]**				**1.500**

[a] LMTO-ASA calculation, [26]
[b]FP LMTO calculations, using seven-layer slabs, [27]
[c] FCD calculations, [28]
Tight-binding total-energy calculations, .[29]
[e] Modified embedded atom calculations, [30]
[f] Embedded atom calculations for FCC metals, [31]
[g] Embedded atom calculations for FCC metals, [32]
[h] Modified analytical embedded atom method calculations, .[33]
Experimental surface energies tabulated by deBoer et al. [34]

5.0 Conclusion

We have in this study employed the new analytical equivalent crystal theory method to provide a set of surface energy for fcc metals. In this work three surfaces were considered for the thirteen fcc metals. These are the (100), (110) and the (111) surfaces. We have successfully extended the surface energy results of the AECT method first proposed by Zypman and Ferrante for fcc from seven to thirteen fcc metals. We have also extended the surface energy results from the (100) face to include the (110) and (111) faces.

The surface energies of the thirteen fcc metals were found to be in good agreement with the available first principles and experimental data. Energies of the fcc metals are uniformly larger than the corresponding results from the EAM, MEAM, MAEAM and tight binding (TB) model, in agreement with experiment. Further, it has been found that the surface energy results from this study consistently support the trend, $\sigma_{111} < \sigma_{100} < \sigma_{110}$ for fcc metals, which then shows that the densest packed fcc (111) surface posses the lowest energy..

In this study the effect of relaxation on the calculated surface energies is ignored. According to the first principles work by Feibelman [22] and by Mansfield et al. [23] , the effect of relaxation on the calculated surface energy of a particular crystal facet may vary from 2% to 5% depending on the roughness. Therefore the neglect of relaxation in this study has little effect on the accuracy of the calculated surface energies.

Acknowledgement

The author would like to acknowledge fruitful discussion with Dr. S.O. Azi on the computation.

References

[1] Zhang J M, Li H Y and Xu K.W J. Phys. Chem. Solids **67** 2006 1623
[2] Zhang J M, Shu Y and Xu K W Appl. Surf. Sci. **252** 2006 5207
[3] Zhang J.M, and Xu K W Chin. Phys**. 13** 2004 205
[4] Zhang J M, Xu K W and Ji V Appl. Surf. Sci. **185** 2002 177
[5] Zhang J M, Xu K W and Ji V Appl. Surf. Sci. **187** 2002 60

[6] Lee N D J. Mater. Sci. **24** 1989 4375
[7] Lee N D J. Mater. Sci. **34** 1999 2575
[8] Smith J R, Perry T, Banerjea A, Ferrante J and Bozzolo G Phys. Rev. B **44** 1991 6444
[9] Foiles S M, Baskes M I and Daws M S Phys. Rev. B **33** 1986 7893
[10] Finnis M W and Sinclair J E Philos. Mag. A **50** 1984 45
[11] Jacobsen K W, Norskov J K and Puska M J Phys. Rev. B **35** 1987 7423
[12] Khare S V and Einstein T L Surf. Sci. **314** 1994 857
[13] Rodriguez A M, Bozzolo G and Ferrante J Surf. Sci. **289** 1993 100
[14] Bozzolo G, Ferrante J Smith J R Phys. Rev. B **45** 1992 493
[15] Bozzolo G, Garces J E, Noebe R D and Farias D Nanotechnology **14** 2003 939
[16] Frenkel A I, Menard L D, Northrup P, Rodriguez j A, Zypman F, Glasner D, Gao S. P, Xu H, YangJ C and Nuzzo R G in: B. Hedman, P.Pianetta (Eds), X-ray Absorption Fine Structure-XAFS13, Vol.**882**, American Institute of Physics 2007, 749
[17] Aghemenloh E, Idiodi J O A and Azi S O Comput. Mater. Sci. **46** 2009 524
[18] Zypman F R and Ferrante J Comput. Mater. Sci. **42** 2008 659
[19] Rose J H, Ferrante J Smith J R Phys. Rev. Lett. **47** 1981 675
Rose J H, Smith J R, Ferrante J Phys. Rev. B**29** 1984 2963
[20] Chapeau-Blondeau F IEEE Trans. Signal Proc. **50** 2002 2160
[21] Hayes B American Scientist **93** 2005 104
[22] Feibelman P J Phys. Rev. B**46** 1992 2532
[23] Mansfield M, Needs R.J, Phys. Rev. B**43** (1991) 8829
[24] Aghemenloh E, Idiodi J O A, J. Nig. Ass. Math. Phys**. 2** (1998) 271
[25] Aghemenloh E, Surface energy calculation in metallic solids, Ph.D. Thesis, University of Benin, Benin City.
[26] Skriver H L, Rosengaard N M, Phys. Rev. B **46** (1992) 7157
[27] Methfessel M, Hennig D, Scheffler M, Phys. Rev. B **46** (1992) 4816
[28] Vitos L, Ruban A V, Skriver H L, Kollar J, Surf. Sci. **411** (1998) 186
[29] Mehl M J, Papaconstantopoulos D A, Phys. Rev. B **54** (1996) 4519
[30] Foiles S M, Baskes M I, Daw M S, Phys. Rev. B**33** (1986) 7983
[31] Cai J, Ye Y Y, Phys. Rev. B **54** (1996) 8398
[32] Baskes M I, Phys. Rev. B **46** (1992) 2727
[33] Wen Y N, Zhang J M, Solid State Commun. **144** (2007) 163
[34] deBoer F R, Boom R, Mattens W C M, Miedema A R, Niessen A K, in: Cohesion in metals (North-Holland, Amsterdam,1988)